Discovery of γ-ray emission associated with Simeis 147 and PSR J0538+2817

Chongyang Ren, Jian Li

Speaker: Chongyang Ren

Purple Mountain Observatory, CAS
University of Science and Technology of China

Outline

1. LHAASO detection and the two-component morphology

2. Fermi-LAT results and multiwavelength counterparts

3. The compact source, radio filament and local gas

4. Chance coincidence, radiation models and energetics

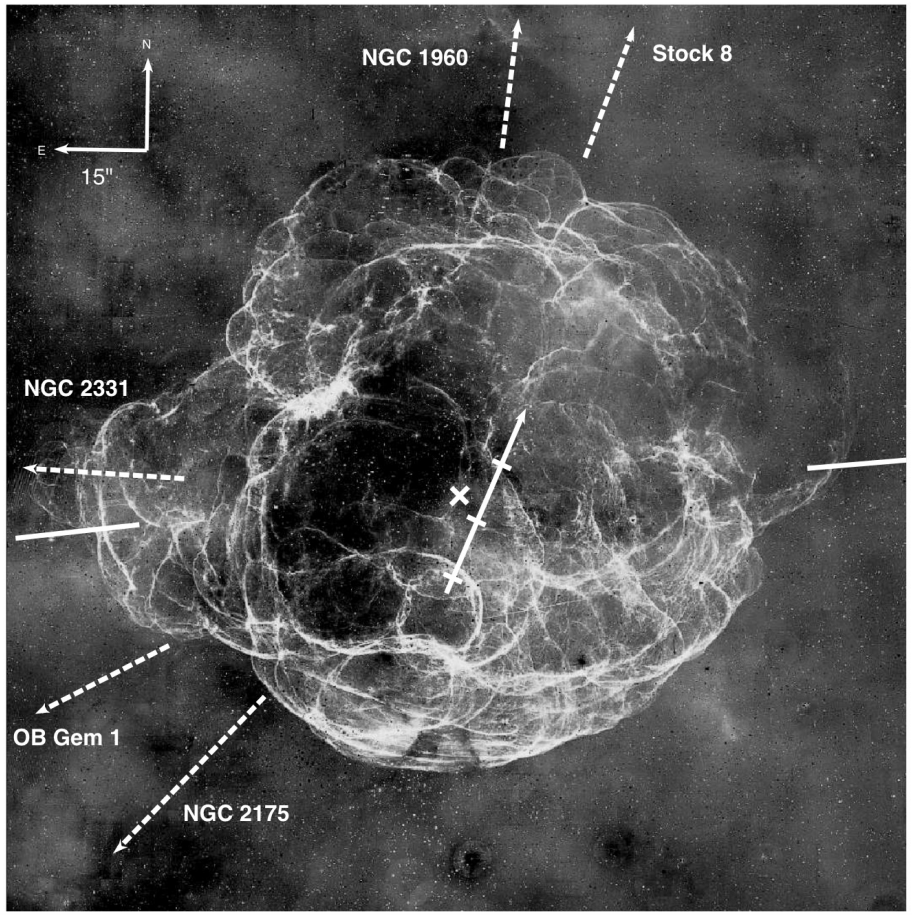
S147 and its pulsar

Simeis 147: SNR G180.0−1.7
An evolved remnant with an angular diameter of ≈3°

PSR J0538+2817 lies inside the remnant.
HD 37424 is a proposed former binary companion.

Arrow tip: pulsar position
Each segment: 20 kyr of proper motion





Hα image: Ng et al., ApJ 654, 487 (2007)

PSR J0538+2817

Parameter	Adopted value
Period	143.16 ms
Spin-down power	$\simeq 5 \times 10^{34}$ erg s^{-1}
Characteristic age	$\simeq$600 kyr
Kinematic age	34.8 ± 0.4 kyr
Parallax distance	$1.47^{+0.42}_{-0.27}$ kpc

Distance: Ng et al., ApJ 654, 487 (2007), VLBA parallax

HAWC observations of the S 147 region

S 147 lies toward the Galactic anticentre ($l \approx 180°$, $b \approx -1.7°$).

HAWC (2019): upper limit

No significant emission in 1128 days.

$F(2\text{–}60\ \text{TeV}) < 1.77 \times 10^{-13}\ \text{cm}^{-2}\ \text{s}^{-1}$

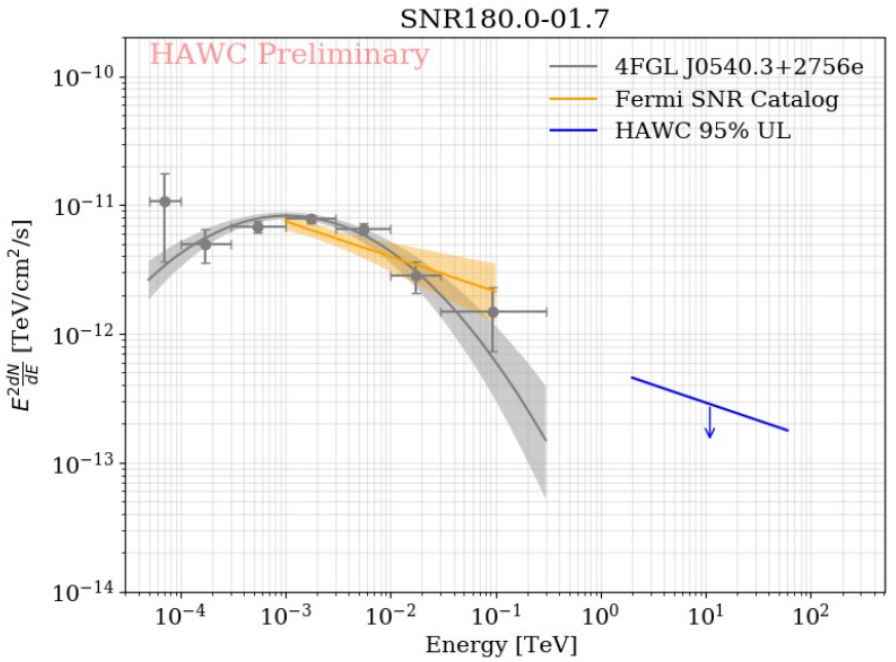
95% CL, uniform disk with $R = 1.5°$, $\Gamma = 2.28$

HAWC (2026): 4HWC detection

4HWC J0538+2804, TS = 27

This source uses a point-source model.

near PSR J0538+2817



2019 S147 SED, Fleischhack, Fig. 1d

The 4HWC result does not separate compact and extended emission.

Fleischhack (2019), arXiv:1907.08575 Alfaro et al. (2026), arXiv:2602.00263

LHAASO data and likelihood analysis

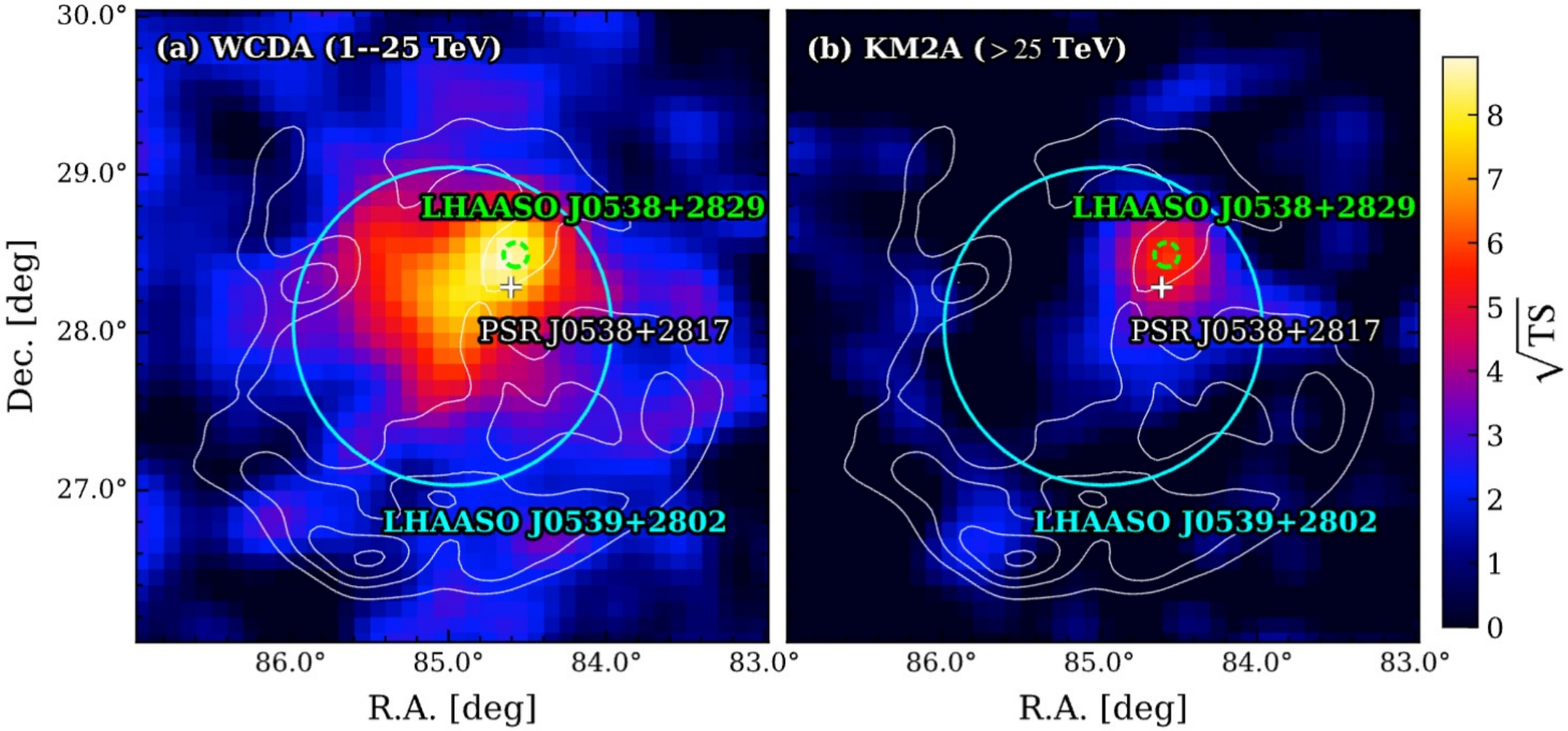
Data	Observation period	Live time	Energy
WCDA	2021 Mar 5 – 2025 Jul 31	1484 days	1.5–25 TeV
KM2A	2019 Dec 27 – 2025 Jul 31	1944 days	>25 TeV

6° × 6° ROI centered on PSR J0538+2817.

Fit morphology and spectrum together with a binned likelihood.

Background: cosmic rays, Galactic diffuse emission
and known sources from the first LHAASO catalogue.

LHAASO TS maps



WCDA shows an extended structure. Separate morphology fits follow.

Morphological model comparison

Data	Model / Component	R.A. (deg)	Decl. (deg)	Γ	σ (deg)	$N_{\rm free}$	ΔTS	ΔAIC
WCDA	1 point	84.61 ± 0.04	28.49 ± 0.04	2.37 ± 0.18	–	4	60.06	0.00
	1 Gaussian	84.82 ± 0.09	28.33 ± 0.08	2.54 ± 0.15	0.40 ± 0.07	5	76.47	−14.41
	1 point	84.60 ± 0.04	28.51 ± 0.04	2.10 ± 0.26	–	9	98.09	−28.03
	1 Gaussian	85.12 ± 0.20	28.10 ± 0.19	2.86 ± 0.14	1.22 ± 0.16	–	–	–
	1 Gaussian	84.60 ± 0.01	28.50 ± 0.01	2.04 ± 0.22	0.07 ± 0.06	10	98.14	−26.08
	1 Gaussian	85.04 ± 0.19	28.11 ± 0.19	2.90 ± 0.15	1.02 ± 0.16	–	–	–
KM2A	1 point	84.53 ± 0.05	28.45 ± 0.05	3.53 ± 0.26	–	4	44.20	0.00
	1 Gaussian	84.53 ± 0.05	28.45 ± 0.05	3.53 ± 0.27	0.02 ± 0.04	5	44.20	2.00

WCDA favors point + Gaussian (ΔAIC = −28.03).

KM2A favors a point source

AIC = 2k − 2 ln L. Reference: one point source for each detector.

Joint fit

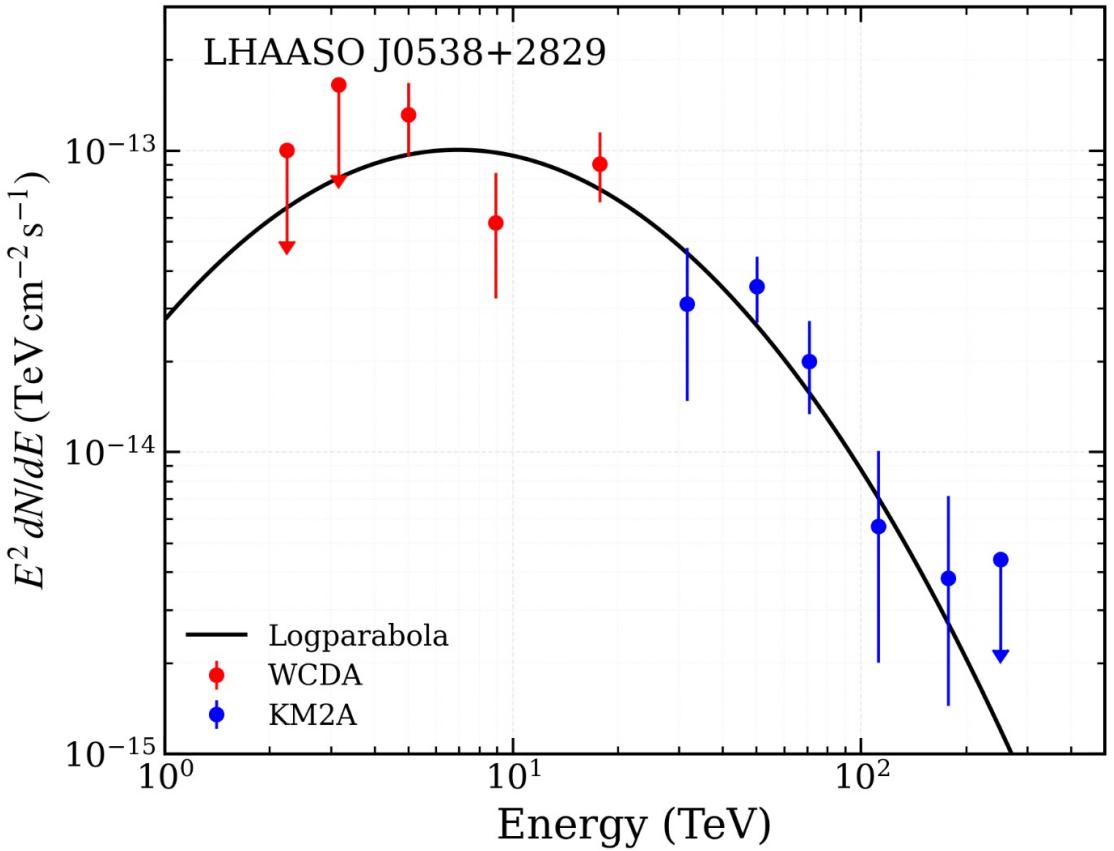
LHAASO J0539+2802 (Gaussian) + LHAASO J0538+2829 (point)

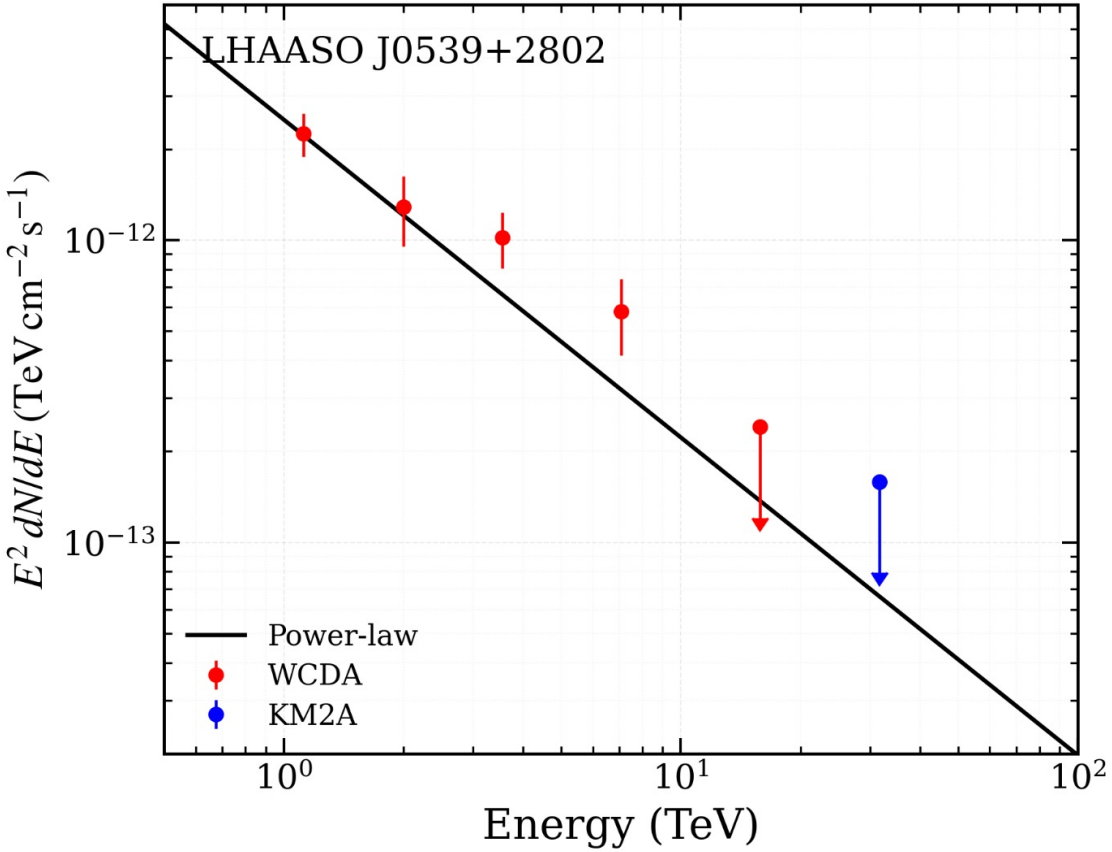
Source / model	R.A. (deg)	Decl. (deg)	σ (deg)	Spectral parameters
J0538+2829 Point + LP	84.57 ± 0.02	28.49 ± 0.03	–	$\alpha = 2.25 \pm 0.23$ $\beta = 0.79 \pm 0.26$
J0539+2802 Gaussian + PL	84.98 ± 0.22	28.04 ± 0.18	1.01 ± 0.34	$\Gamma = 3.05 \pm 0.10$

At 10 TeV: $N_0 = (0.96 \pm 0.18) / (2.22 \pm 1.25) \times 10^{-15}$ TeV^{-1} cm^{-2} s^{-1}
Compact / extended components

Point source: 0.2073° from PSR J0538+2817. Significance: 7.6σ / 5.3σ (point / extended).
LP preferred to PLEC by ΔAIC = 0.77.
Extended source: PL, with no KM2A detection.

LHAASO spectral energy distributions



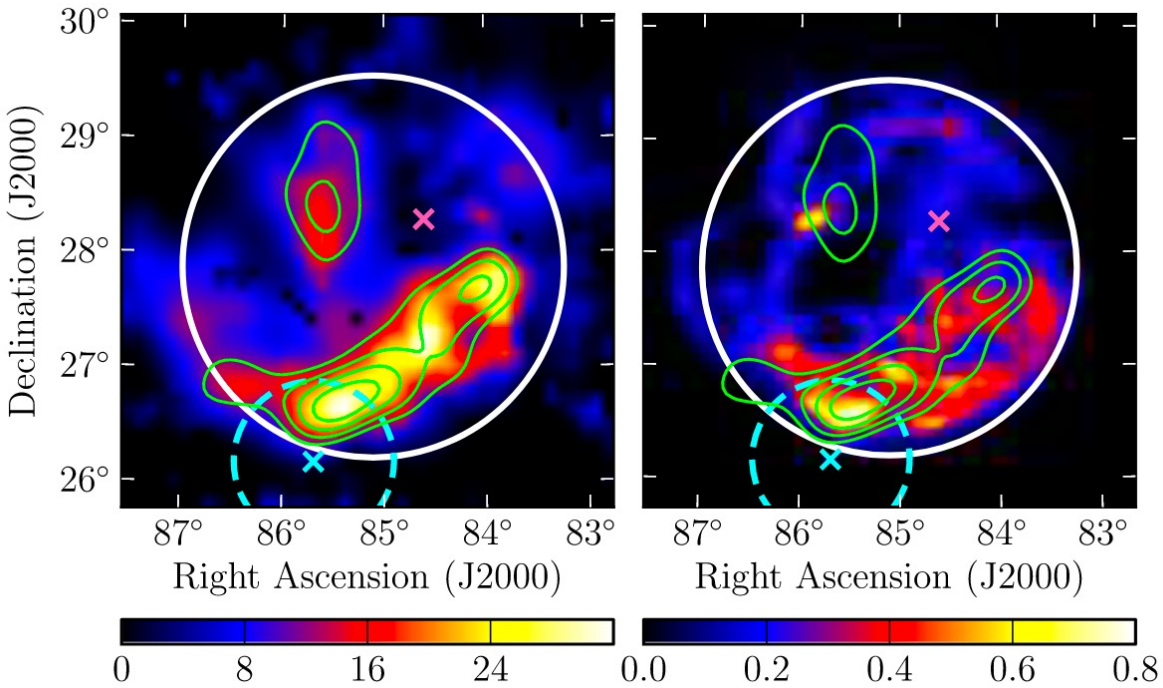


Compact: curved spectrum beyond 100 TeV

Extended: softer spectrum, mainly below 10 TeV

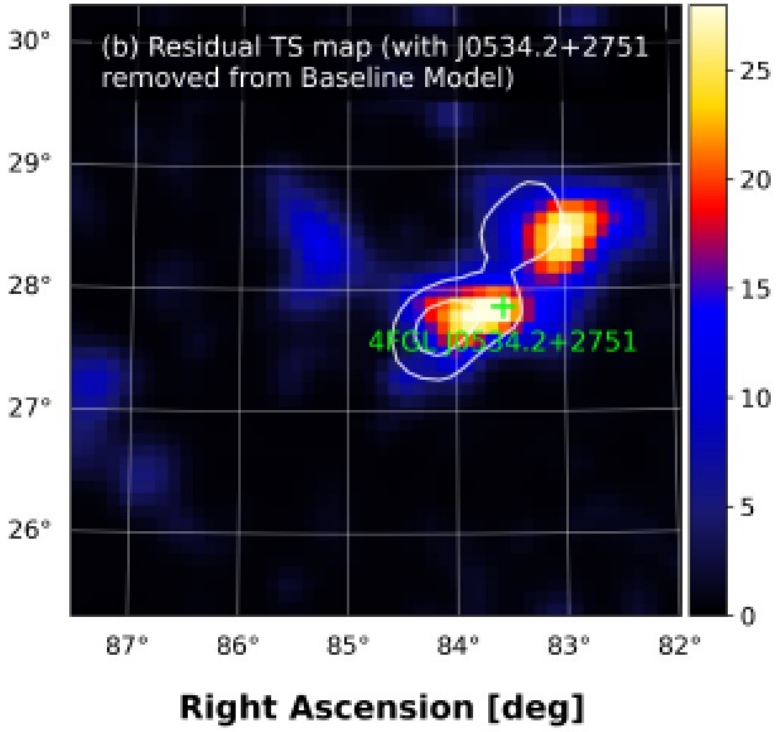
Multiwavelength counterparts: GeV observations

Early LAT: Hα shell.



Katsuta et al., ApJ 752, 135 (2012)

2026: >1 GeV component follows CO (0–5 km s^{-1})



CO / GeV (2026)

Yang et al., arXiv:2601.20210 (2026)

Fermi-LAT analysis

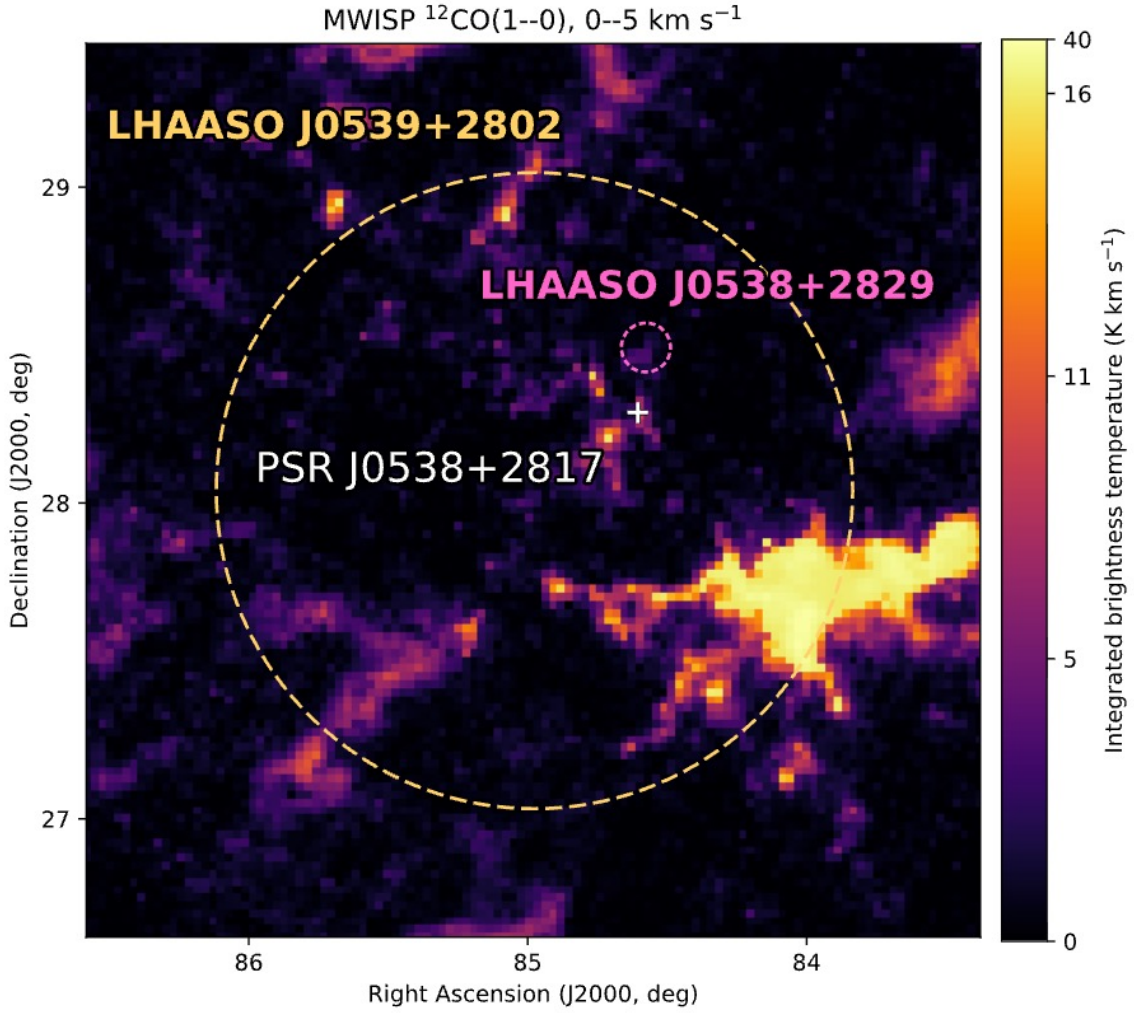
18 years of SOURCE events, 10 GeV–1 TeV.

15° ROI. 3FHL catalogue plus Galactic and isotropic backgrounds.

Free source spectra within 5° and both diffuse normalizations.

Compare disk / Gaussian, CO, H I and Hα templates.

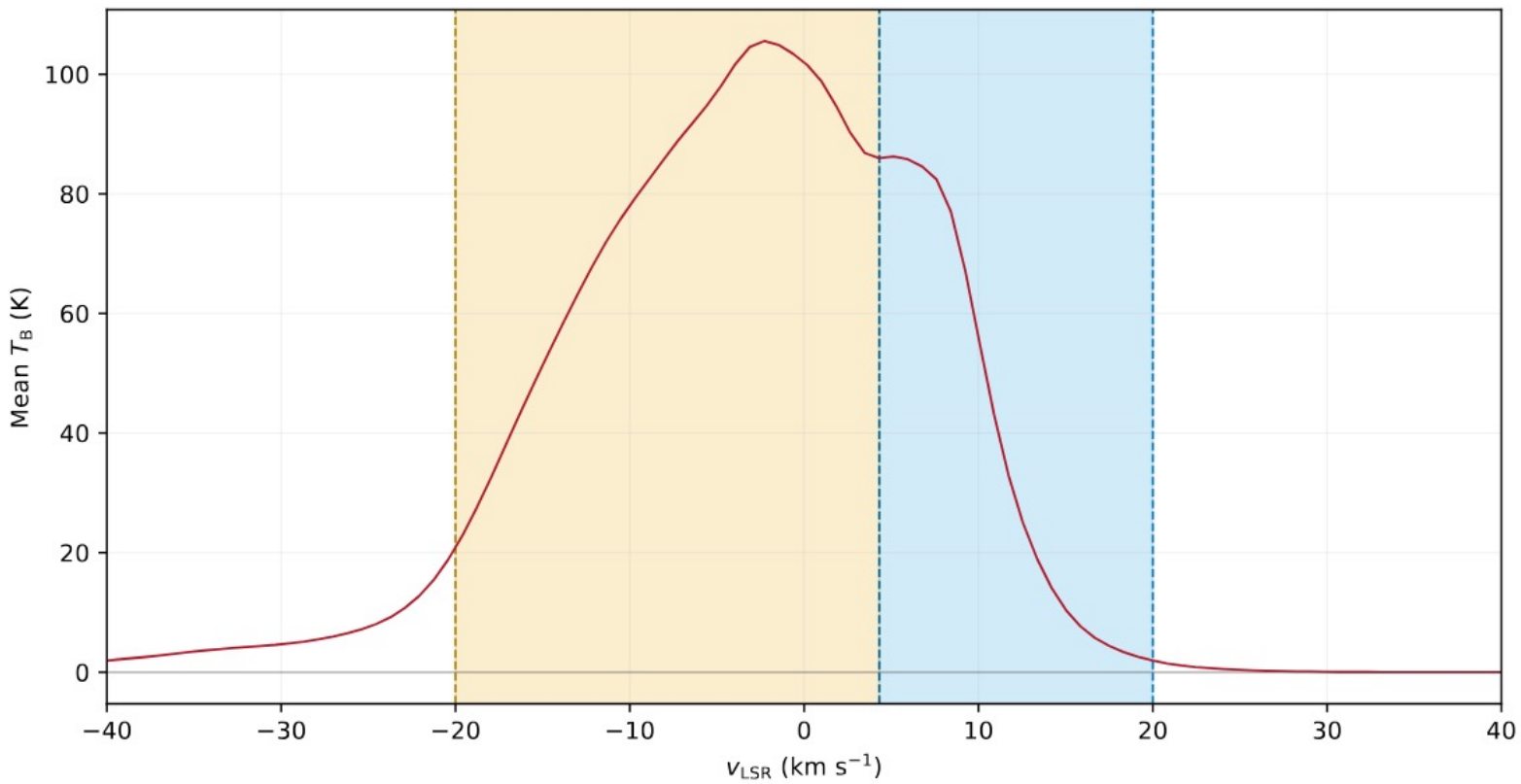
MWISP ^{12}CO: extended region



Gas-template selection (1/3)
CO around J0539+2802

CO integration: 0–5 km s^{-1}
Following the previous S147 study

H I velocity profile

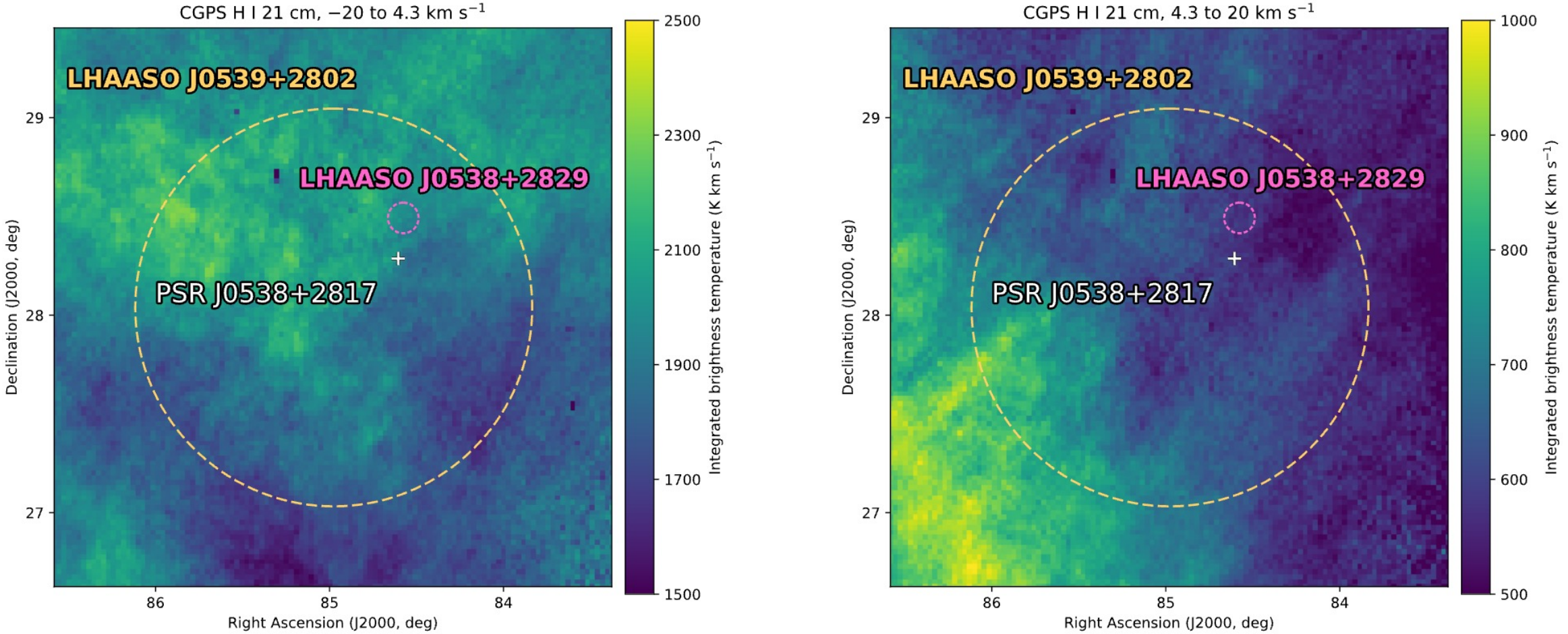


Gas-template selection (2/3)
CGPS 21-cm data

Two broad components:
−20 to +4.3 km s^{-1}
+4.3 to +20 km s^{-1}

The velocity split defines the H I spatial templates.

H I spatial distribution



Gas-template selection (3/3): two H I distributions within the same 2° region.

Fermi-LAT template comparison

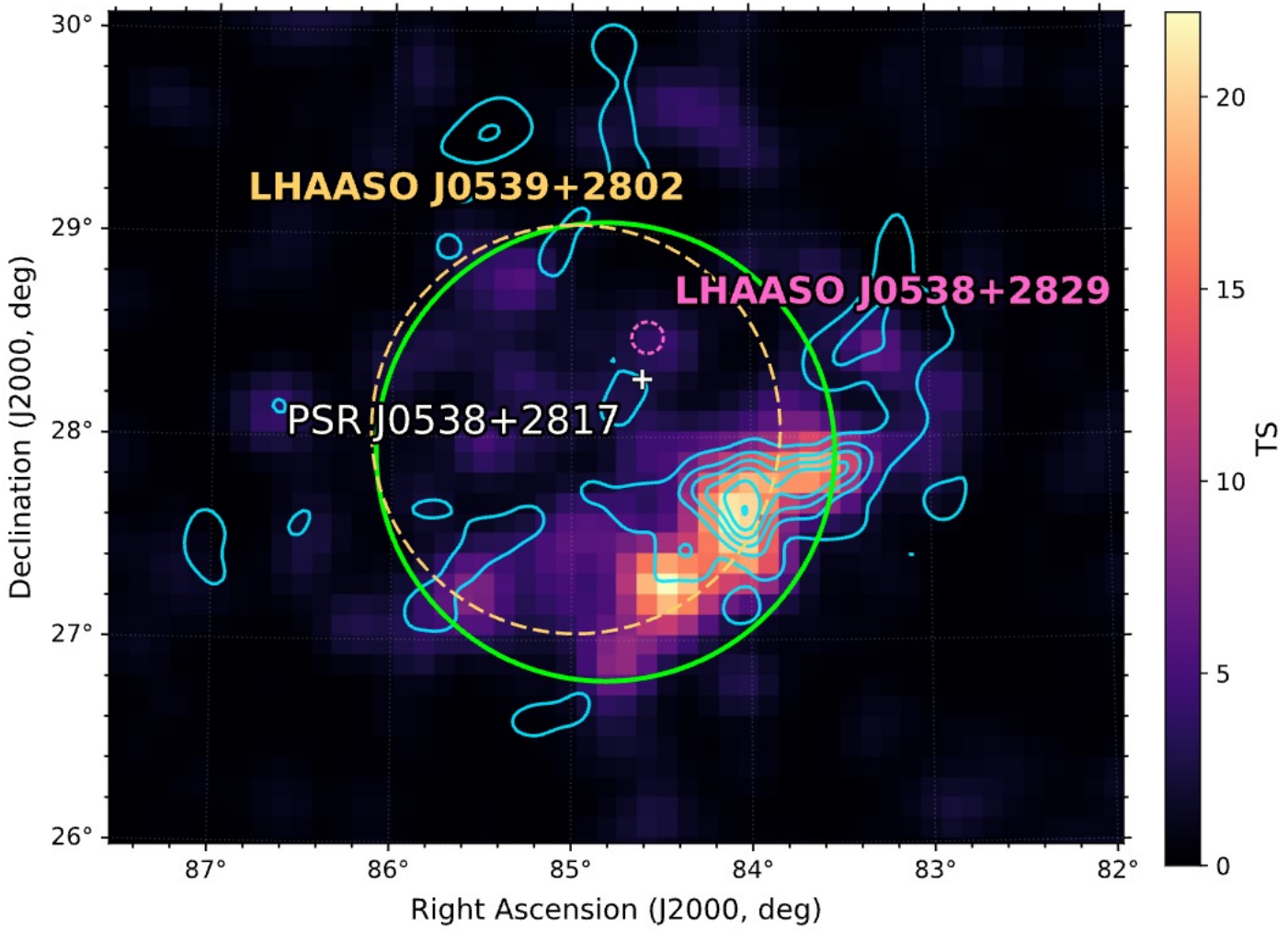
Model	ΔTS	ΔAIC	ΔTS_{geo}	$\Delta TS_{H\alpha}$	$\Delta TS_{H\,I}$	ΔTS_{CO}
CO + disk	0.00	0.00	34.05	–	–	35.57
CO + Gaussian	−1.53	1.53	32.53	–	–	37.90
CO + Hα	−23.07	17.06	–	10.99	–	47.84
CO + Hα + disk	1.38	2.62	24.44	0.91	–	32.80
CO + H I	−29.46	23.46	–	–	4.60	51.70

Best model: CO + disk: TSdisk = 34.05, TSCO = 35.57. Both components are significant.

Additional Hα is insignificant (ΔTS = 0.91).

Component ΔTS: remove that component and refit. Model ΔTS reference: CO + disk.

Fermi-LAT morphology



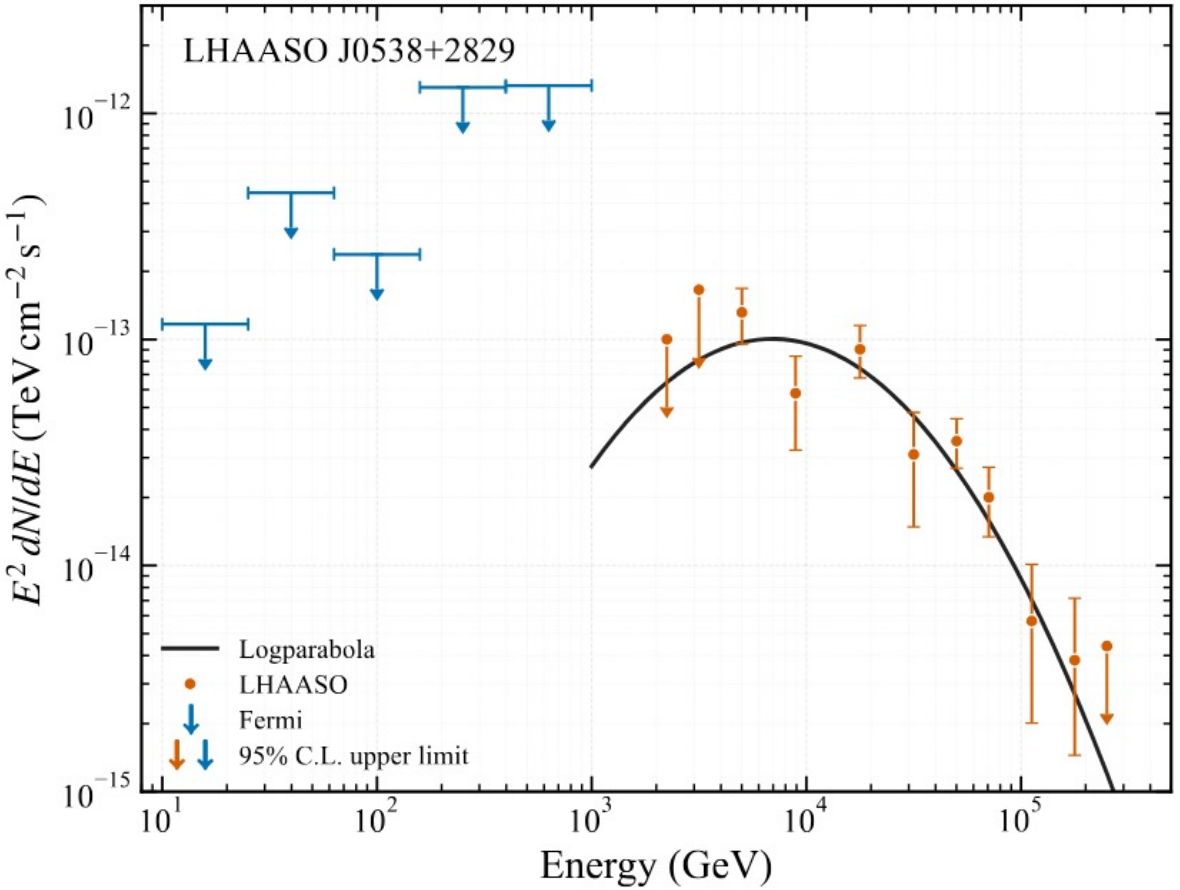
Disk: $\Delta TS = 34.05$
R.A. = 84.81° ± 0.10°
Decl. = 27.93° ± 0.11°
Radius = 1.13° ± 0.07°

The disk center lies 0.19° from LHAASO J0539+2802.

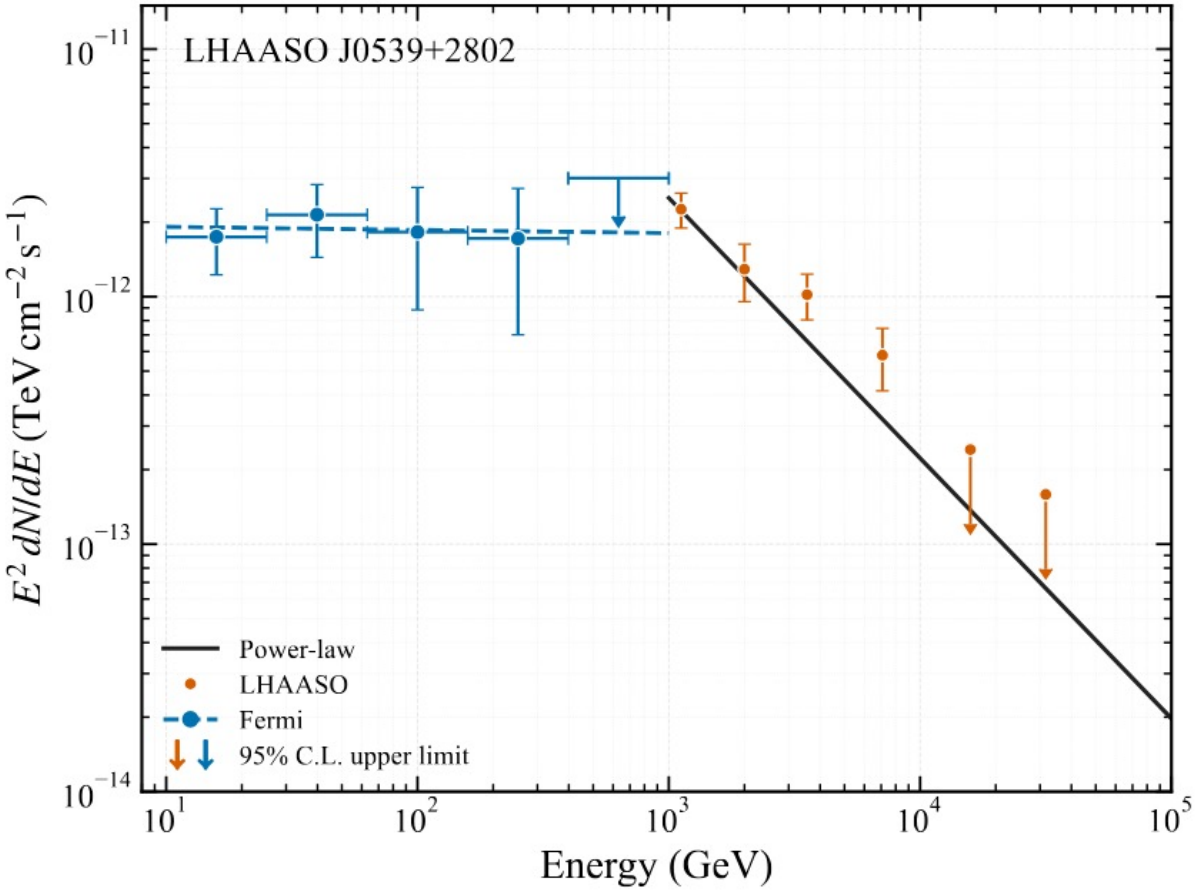
Cyan: CO contours. Green: LAT disk. Gold / magenta: LHAASO extended / point components.

Fermi-LAT and LHAASO SEDs

Point source: no LAT detection



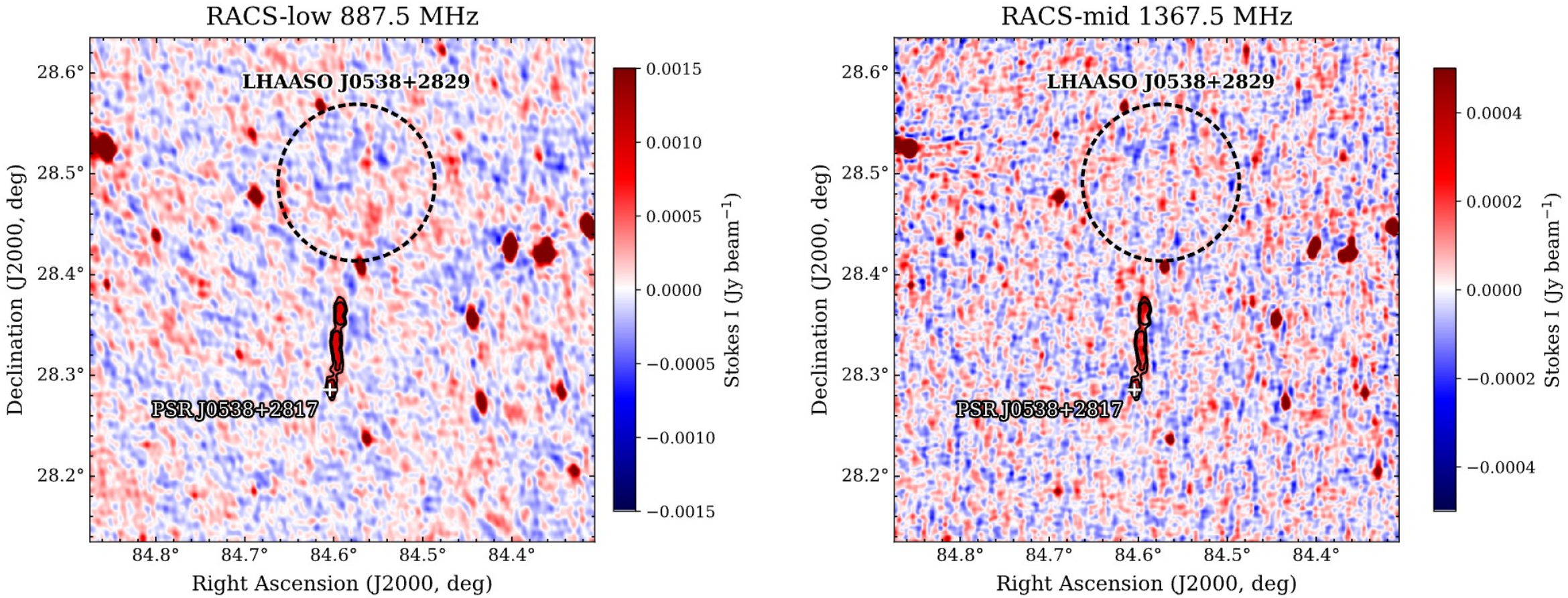
Extended: LAT disk + LHAASO PL



LAT disk: $\Gamma = 2.01 \pm 0.16$, F10 GeV–1 TeV $= (1.37 \pm 0.34) \times 10^{-11}$ erg cm^{-2} s^{-1}

Radio filament and compact TeV localization

The filament extends northward toward LHAASO J0538+2829.



Chance coincidence and directional alignment

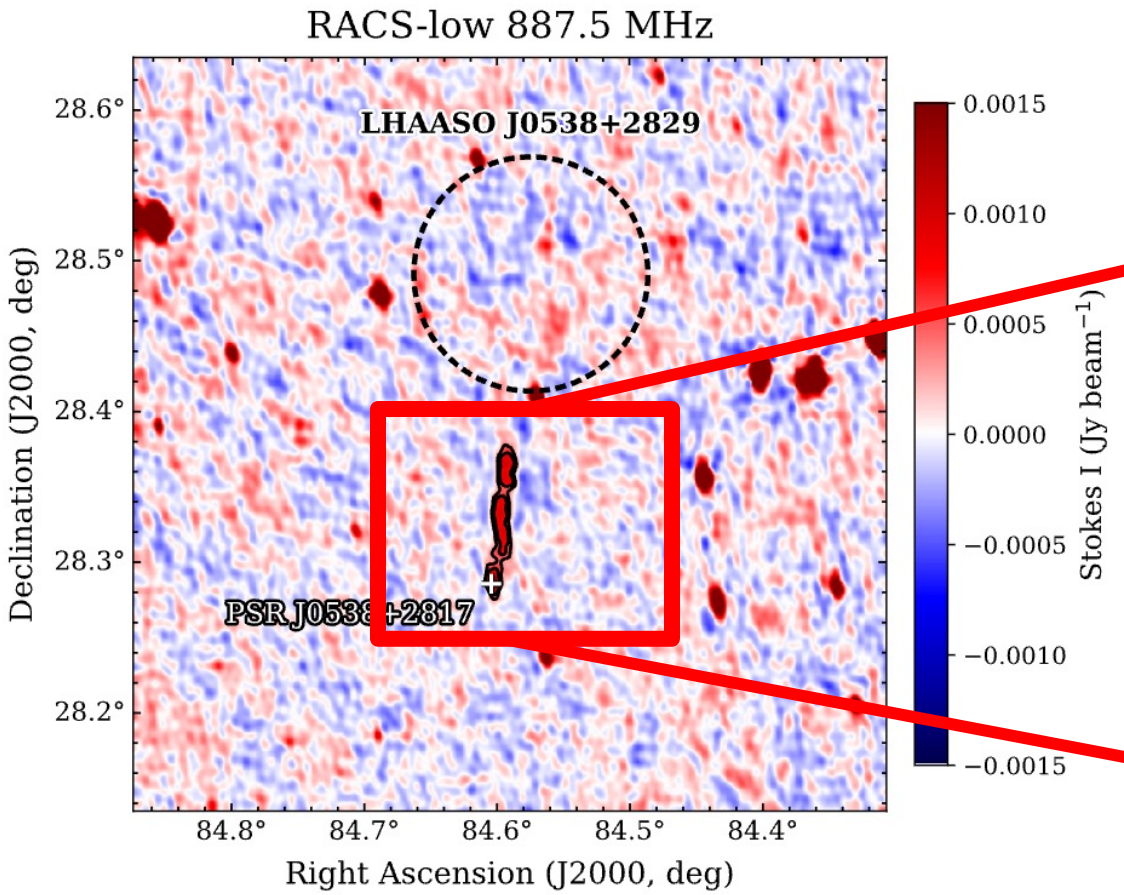
The 99% localization circle subtends 44.02° at the pulsar.
fdir = 44.02° / 360° = 0.1223

Pulsar sample	N	Spatial probability	With alignment
$\dot{E}/D^2 > 10^{34}$	2	0.5090%	0.0622%
All local pulsars	11	2.7678%	0.3384%

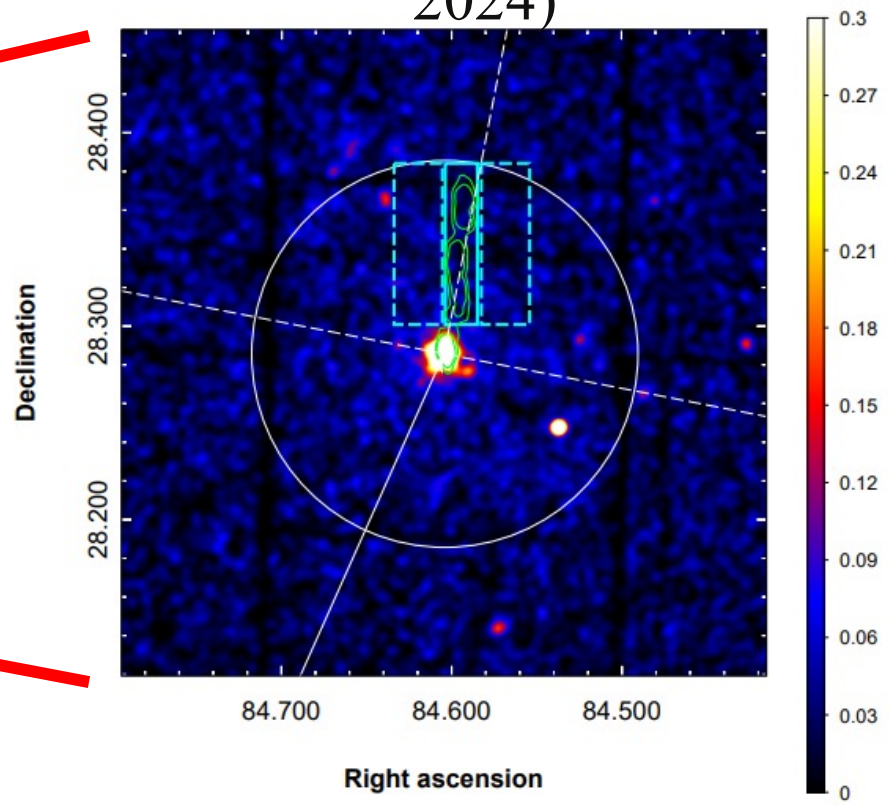
The UHE source LHAASO J0538+2829 is very likely associated with PSR J0538+2817

Uniform local pulsar density and independent orientations.

Radio filament and compact TeV localization



No X-ray detection of the filament. (XMM-Newton, 0.5-3 keV; Khabibullin et al. 2024)



Radio filament and compact TeV localization

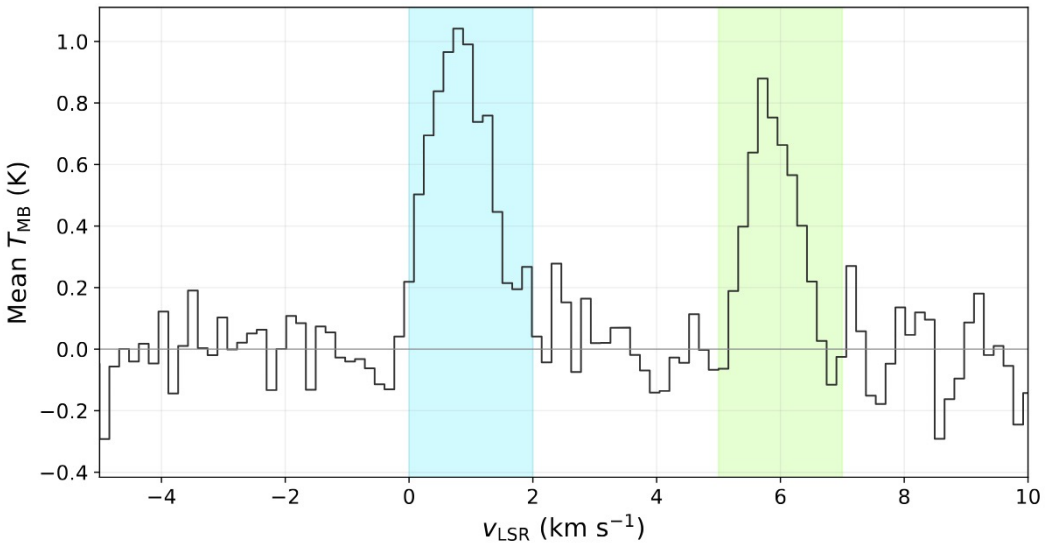
Radio emission of the filament and corresponding no X-ray detection, give a lower limit of the magnetic field > 40 nG (Khabibullin et al. 2024).

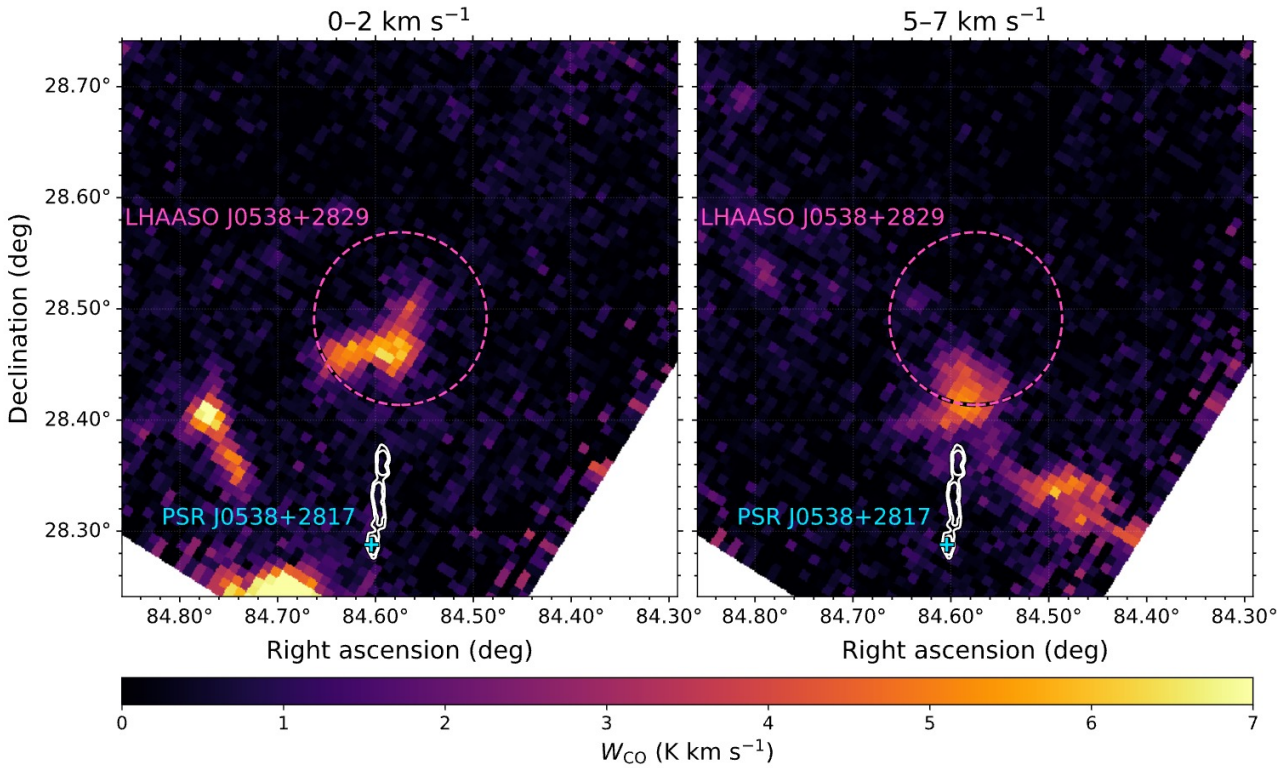
Electrons emitting the 1GHz radio filament would have a $\gamma \sim 10^5$.

If we assume LHAASO J0538+2829 is powered by PSR J0538+2817 with particles transported through the filament, these electrons could not produce UHE gamma-rays we observed through IC between CMB and FIR (30 K, 0.5 eV cm^{-3}), NIR (3000 K, 1.0 eV cm^{-3}) photons.

MWISP ^{12}CO: compact region

CO spectrum within the 99% localization region of LHAASO J0538+2829





Two velocity components: 0–2 and 5–7 km s^{-1}

Compact-source SED modeling

naima at d = 1.47 kpc, using the joint WCDA–KM2A SED

$$\frac{dN}{dE} = A\left(\frac{E}{E_0}\right)^{-\alpha} \exp\left(-\frac{E}{E_{\rm cut}}\right), \qquad E_0 = 1\,\mathrm{TeV}$$

Free parameters: particle energy W, index α and cutoff energy.
Normalize W over 1 TeV–10 PeV, also report 1 GeV–10 PeV.

Fit detected γ-ray points, with LAT / LHAASO limits as constraints.
Compare χ^2 on detections: 5 degrees of freedom.

XMM-Newton MOS1 + MOS2, observation 0112200401, ≈17 ks.
No significant X-ray emission in the compact TeV localization.

95% limits: LAT $<9.38 \times 10^{-13}$ (10 GeV–1 TeV)
XMM-Newton $<3.4 \times 10^{-12}$ (0.2–10 keV), in erg cm^{-2} s^{-1}

Leptonic and hadronic model assumptions

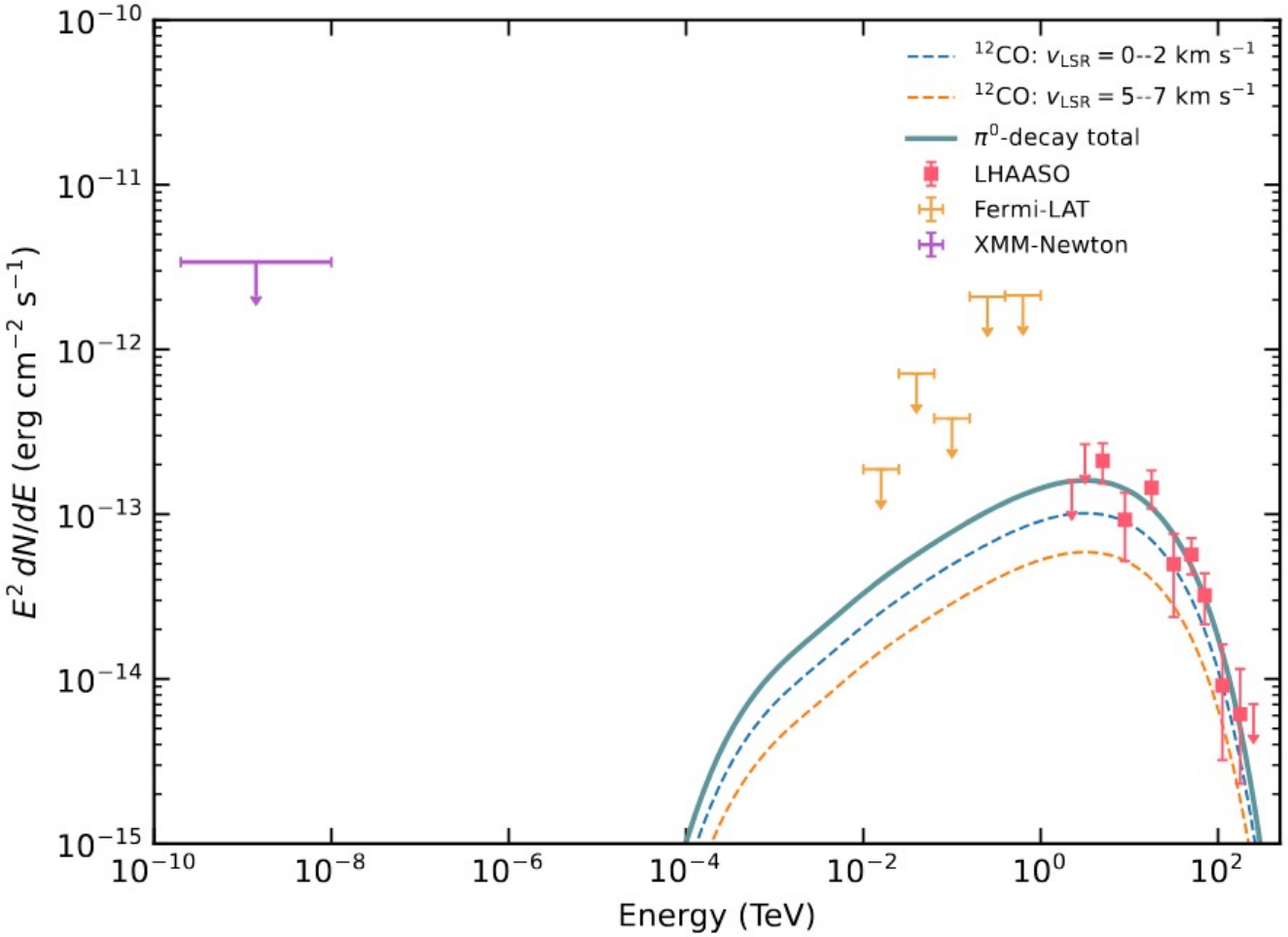
Leptonic: Inverse Compton + synchrotron
electrons with a $\gamma \sim 10^8$, which is inconsistent with particles transported by the filament

Target photons: CMB, FIR (30 K, 0.5 eV cm^{-3}), NIR (3000 K, 1.0 eV cm^{-3}).

Hadronic: proton interactions and π^0 decay

Target	Density (cm^{-3})	Particle normalization
0–2 km s^{-1} cloud	37.34	Separate proton fit
5–7 km s^{-1} cloud	21.67	Separate proton fit
Combined two clouds	59.01	Shared proton spectrum and W_p

Broadband hadronic



Both scenarios fit the γ-ray SED (χ^2/dof ≈5.1/5).

Fixed electron spectrum: synchrotron reaches the plotted XMM limit at B ≈16.1 μG.

Best-fit particle parameters

d = 1.47 kpc. Particle energies in erg

Model	α	$E_{\rm cut}$ (TeV)	W (1 GeV–10 PeV)	W (1 TeV–10 PeV)	χ^2/dof
Leptonic (W_e)	2.353	83.58	1.35×10^{46}	8.60×10^{44}	5.109/5
Hadronic 0–2 km s^{-1}	1.624	164.25	1.85×10^{46}	1.57×10^{46}	5.100/5
Hadronic 5–7 km s^{-1}	1.642	167.21	3.28×10^{46}	2.73×10^{46}	5.091/5
Hadronic combined	1.664	174.79	1.23×10^{46}	1.01×10^{46}	5.097/5

Hadronic fits: proton index ≈1.6, cutoff ≈165–175 TeV.

The γ-ray SED allows both radiation scenarios.

Particle energy budget

Reference scale: Ėnow tkin = 5.49 × 10^{46} erg
Ėnow = 5 × 10^{34} erg s^{-1}, tkin = 34.8 kyr

Model	$W_{1\,\mathrm{GeV}-10\,\mathrm{PeV}}/(\dot{E}_{\mathrm{now}}t_{\mathrm{kin}})$	$W_{1\,\mathrm{TeV}-10\,\mathrm{PeV}}/(\dot{E}_{\mathrm{now}}t_{\mathrm{kin}})$
Leptonic (W_e)	24.50%	1.57%
Hadronic 0–2 km s^{-1}	33.74%	28.53%
Hadronic 5–7 km s^{-1}	59.76%	49.79%
Hadronic combined	22.38%	18.32%

Above 1 TeV: leptonic 1.57%, combined hadronic 18.32%.

Particle transport and possible origin

Projected pulsar–TeV separation: 5.3 pc at 1.47 kpc.

The radio filament points toward the compact TeV source, which could be the path for particle transportation.

Nearby CO gas provides possible targets for escaped protons.

Both leptonic and hadronic processes can explain the compact-source SED.

Conclusions

First LHAASO detection of γ-ray emission in the S147 region.
Two components: LHAASO J0538+2829 and LHAASO J0539+2802.

J0539+2802: extended emission inside S147.
The LAT component agrees in position and spectrum.

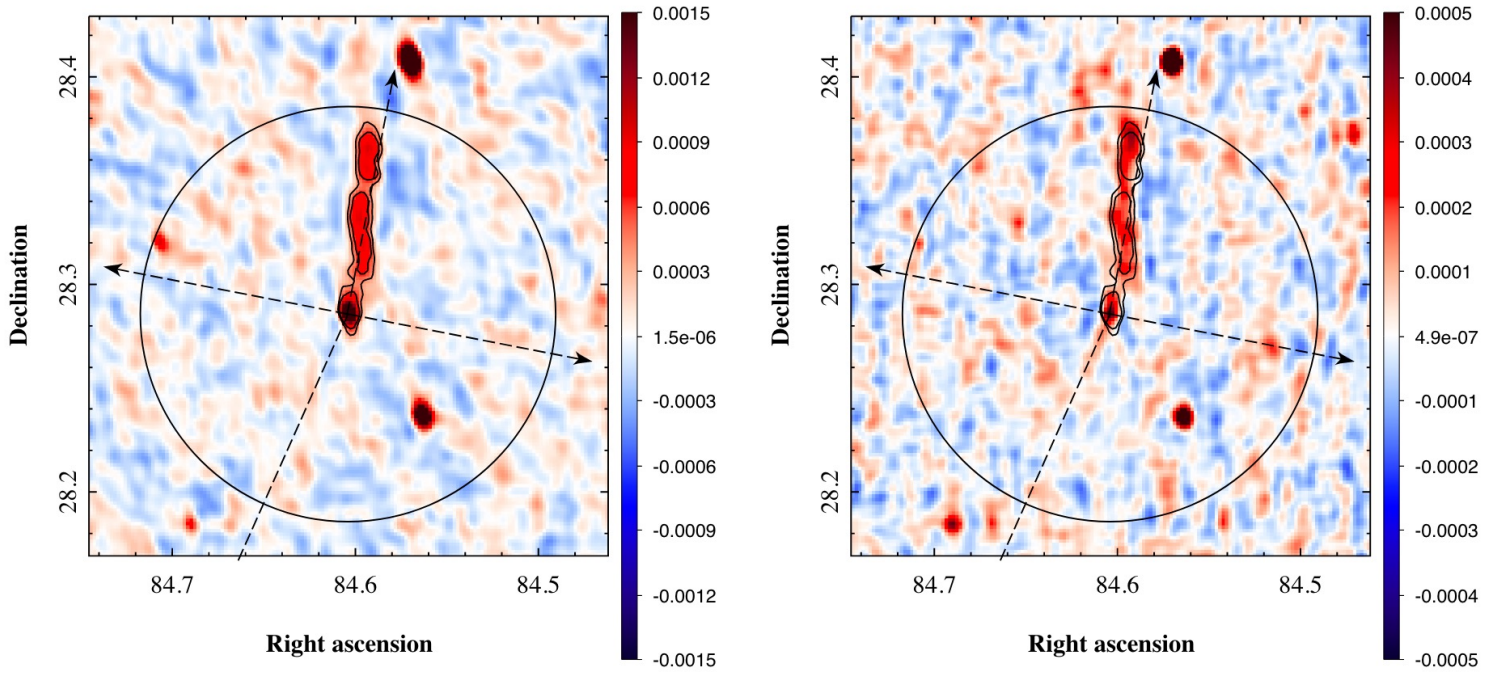
J0538+2829: emission beyond 100 TeV near the pulsar radio filament.
Both leptonic and hadronic processes fit the SED.

Surrounding gas provides possible targets for hadronic emission.
The radio filament suggests collimated outflow or anisotropic particle transport.

The one-sided radio filament

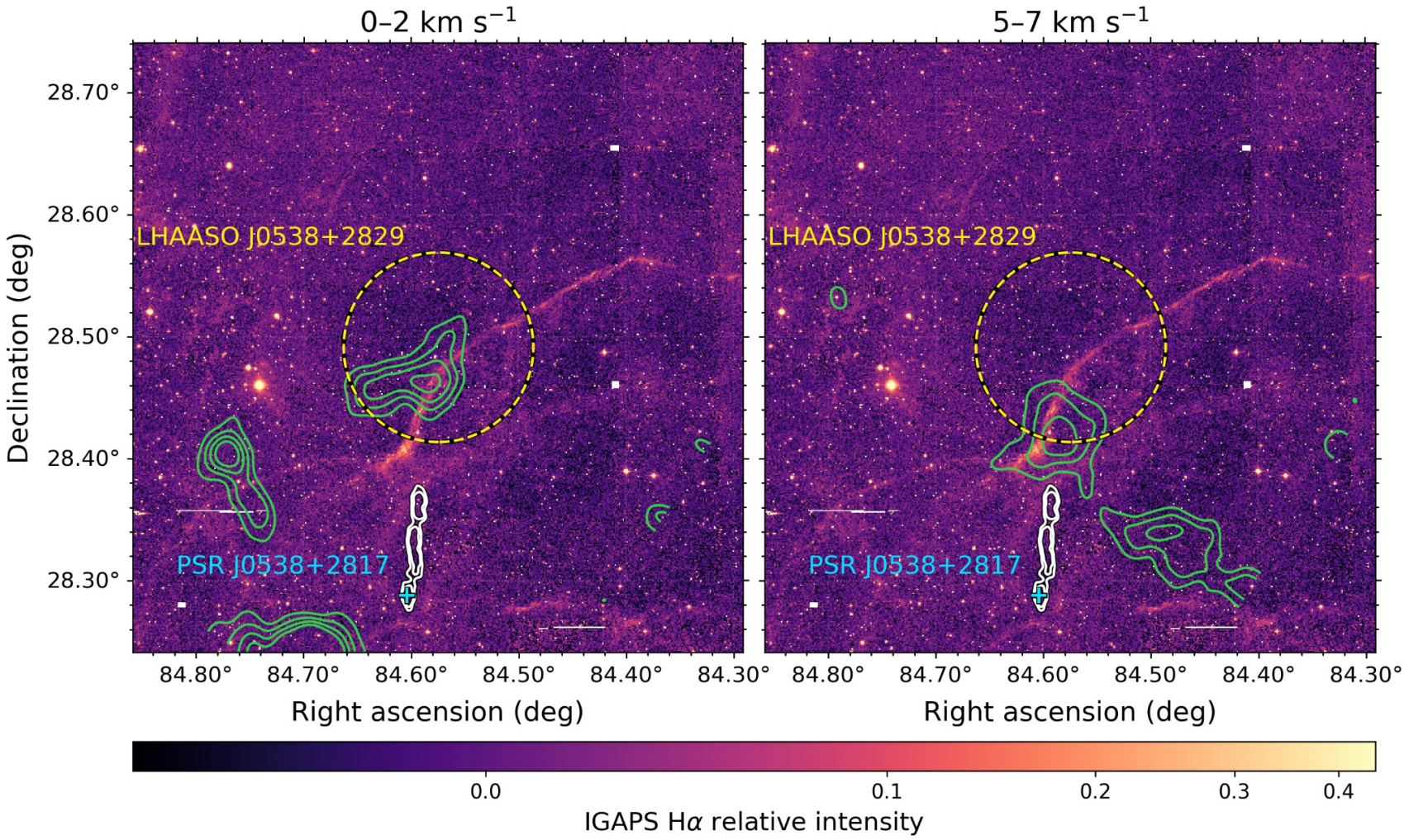
The filament lies ahead of the pulsar along its direction of motion.

Within ≈17° of proper motion, and nearly perpendicular to the X-ray structure.



Discovery of a one-sided radio filament of PSR J0538+2817 in S147
Khabibullin et al. (2024), MNRAS 527, 5683–5692. doi:10.1093/mnras/stad3452

Hα filaments and molecular gas



IGAPS Hα background
Green: CO contours
White: radio filament

CO and Hα overlap the compact TeV region, providing possible targets.

The optical and radio filaments are distinct.

Chance-coincidence calculation

Pulsar–TeV separation: $d\theta = 0.2073°$.

Local window: $20° \times 5° = 100\ \mathrm{deg}^2$.
11 pulsars, including 2 with $\dot{E} / D^2 > 10^{34}\ \mathrm{erg\ s^{-1}\ kpc^{-2}}$.

99% localization radius: $R_{99} = 0.0777°$.
Search radius: $r = d\theta + R_{99} = 0.2850°$.

$$\mathbf{P = 1 - \exp[-\pi\rho\,(d\theta + R_{99})^2],} \qquad \mathbf{\rho = N / 100\ deg^2}$$

ATNF v2.8.1. Local Poisson prescription following Cao et al., arXiv:2502.15447.

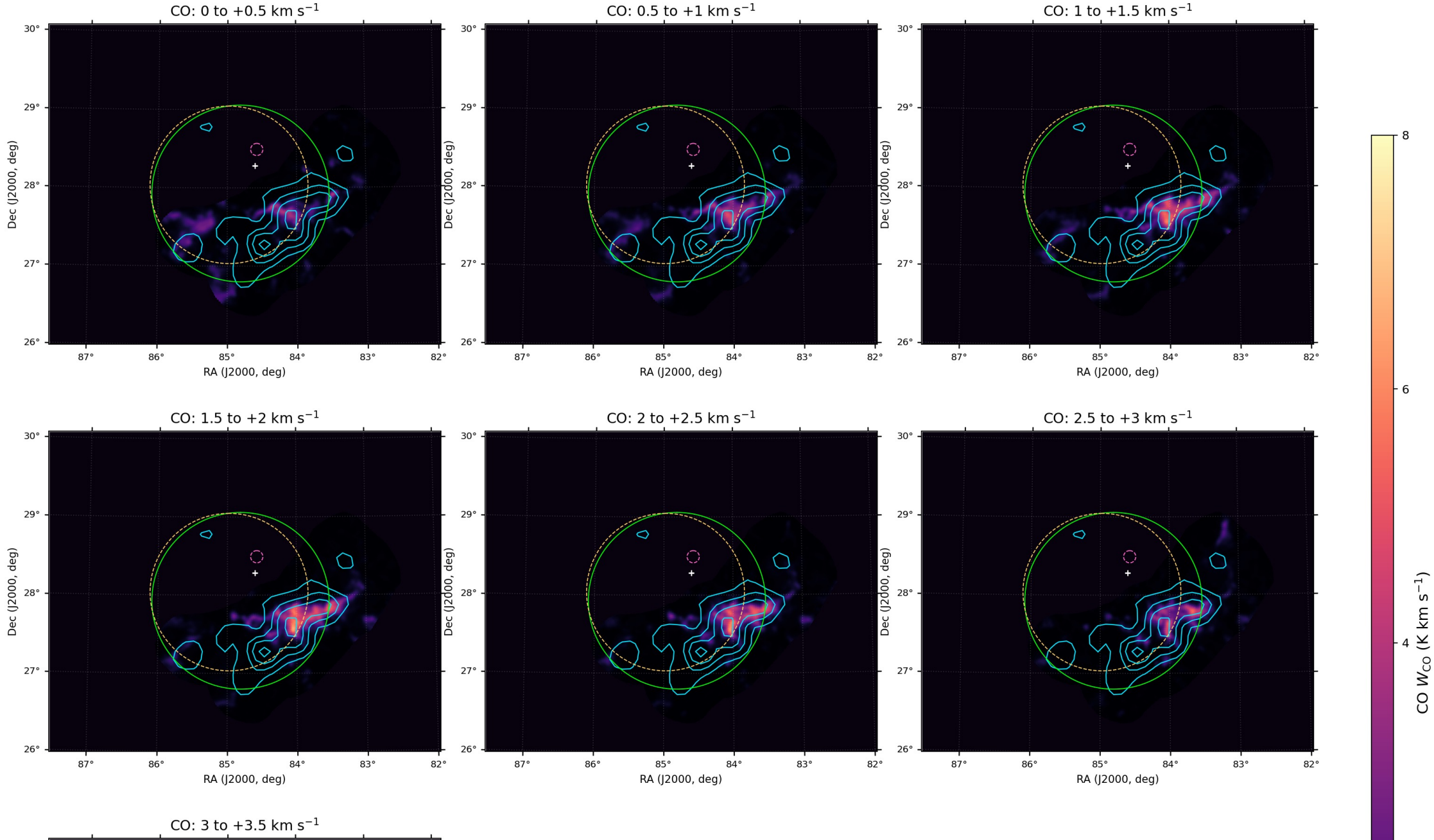
Best-fit particle parameters

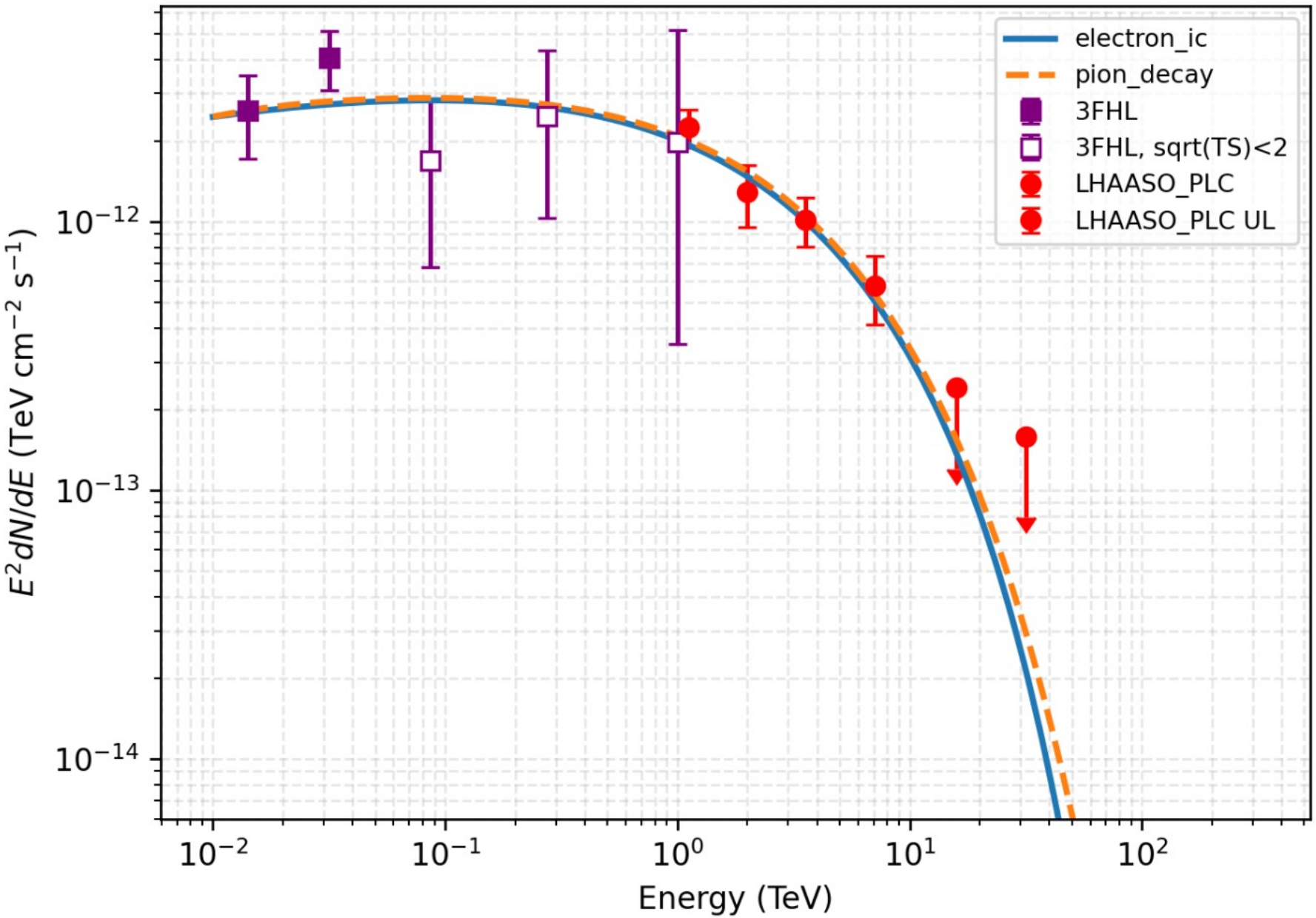
d = 1.47 kpc. Particle energies in erg

Model	α	$E_{\rm cut}$ (TeV)	W (1 GeV–10 PeV)	W (1 TeV–10 PeV)	χ^2/dof
Leptonic (W_e)	2.353	83.58	1.35×10^{46}	8.60×10^{44}	5.109/5
Hadronic 0–2 km s^{-1}	1.624	164.25	1.85×10^{46}	1.57×10^{46}	5.100/5
Hadronic 5–7 km s^{-1}	1.642	167.21	3.28×10^{46}	2.73×10^{46}	5.091/5
Hadronic combined	1.664	174.79	1.23×10^{46}	1.01×10^{46}	5.097/5

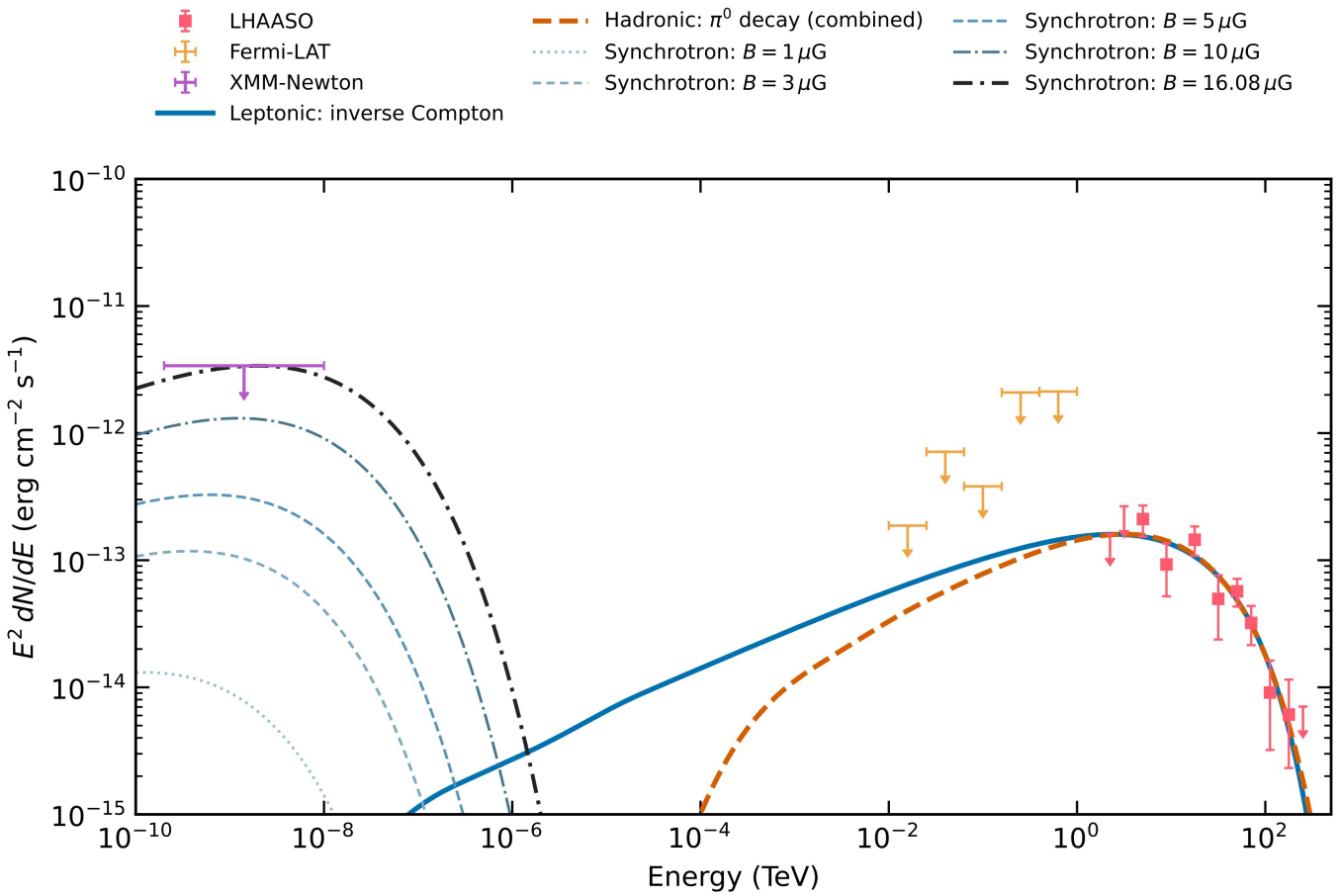
Hadronic fits: proton index ≈1.6, cutoff ≈165–175 TeV.

The γ-ray SED allows both radiation scenarios.


CO: 0 to +0.5 km s^{-1}
CO: 0.5 to +1 km s^{-1}
CO: 1 to +1.5 km s^{-1}
CO: 1.5 to +2 km s^{-1}
CO: 2 to +2.5 km s^{-1}
CO: 2.5 to +3 km s^{-1}
CO: 3 to +3.5 km s^{-1}
Dec (J2000, deg)
RA (J2000, deg)
30°
29°
28°
27°
26°
87°
86°
85°
84°
83°
82°
CO W_{CO} (K km s^{-1})
8
6
4


electron_ic
pion_decay
3FHL
3FHL, sqrt(TS)<2
LHAASO_PLC
LHAASO_PLC UL
E^2dN/dE (TeV cm^{-2} s^{-1})
10^{-12}
10^{-13}
10^{-14}
10^{-2}
10^{-1}
10^{0}
10^{1}
10^{2}
Energy (TeV)

Broadband leptonic–hadronic comparison



Both scenarios fit the γ-ray SED (χ^2/dof ≈5.1/5).

Fixed electron spectrum: synchrotron reaches the plotted XMM limit at B ≈16.1 μG.